

Behzad Shirkavand Hadavand and Hossein Hosseini\*

# Investigation of viscoelastic properties and thermal behavior of photocurable epoxy acrylate nanocomposites

DOI 10.1515/secm-2015-0161

Received April 17, 2015; accepted February 26, 2016

**Abstract:** In this study, the dynamic-mechanical properties and thermal behavior of the nanocomposites of a photocurable epoxy-acrylate resin and CuO nanohybrid were determined. In order to improve the dispersion of CuO nanoparticles and prevention of nanoparticle migration to the surface coating, the surface of commercial nanoparticles was modified by triethoxymethylsilane (TEMS) and vinyltrimethoxysilane (VTMS) as silane-coupling agents. Dynamic mechanical analysis (DMA), thermogravimetric analysis (TGA), and differential scanning calorimetry (DSC) tests were then performed on CuO-filled epoxy-acrylate resins to identify the loading effect on the properties of material. The thermal stability of nanocomposites was affected slightly after incorporation of CuO nanoparticles. DMA studies revealed that filling the CuO nanoparticles into epoxy-acrylate resin can produce a significant enhancement in storage modulus, as well as a shift in the glass transition temperature. The films reinforced with the modified CuO exhibit the most significant enhancements in properties.

**Keywords:** nanocomposite; photocurable epoxy acrylate resins; thermal behavior; viscoelastic properties.

## 1 Introduction

Epoxy resins are mainly used in coatings and structural applications. The proper selection of curing agent affects specific proficiency characteristics of the cured epoxy resin. The cured epoxy resins represent good adhesion to a variety of substrates. High adhesion performance of cured epoxy resin is because of the polar hydroxyl and

ether groups in the backbone structure of epoxy resins [1, 2]. The mechanical and thermal properties of cured epoxy resins severely depend on the chemical nature of the epoxy resins, cross-linker, and the concentration and type of curing agent.

On the other hand, in the recent years, the use of photocurable or ultraviolet (UV) curable coatings has been increased. UV curing means that the process of photo-initiated conversion of oligomers from a liquid to a solid is a popular alternative to conventional thermal curing. The process of UV curing has many advantages such as high-speed process, low-energy consumption, and environment-friendly characteristics [3–7]. In many applications, it is necessary to have thin film for coatings and UV-curing systems that are suitable for this purpose.

The common oligomers used in UV-curable systems are epoxy acrylates and urethane acrylates resins [8–10]. For preparing epoxy acrylate, epoxy resin reacted with acrylated materials, such as methacrylic acid or methyl methacrylate, in the presence of a catalyst [8] to achieve a UV-curable epoxy oligomer.

As epoxy resins like other thermosetting polymers are extremely brittle, which limits their applications in products that require high impact and scratch strength, recently, nanoparticles have been used in cured epoxy resins to enhance the physical-mechanical properties of these coatings. Different types of nanoparticles such as  $Al_2O_3$ , silica, clay, carbon nanotube, and  $TiO_2$  are used to enhance the physical-mechanical characteristics of the epoxy resins [11–14]. Several mechanisms for improvement of the physical-mechanical characteristics of nano-filled epoxy resins have been suggested. These mechanisms are crack deflection, crack pinning, and de-bonding [15, 16]. Notwithstanding the good properties of nanoparticles, the physical-mechanical properties of nano-filled epoxy resins are not enhanced significantly. In order to attain maximum improvement of the mechanical properties of nano-filled epoxy resins, homogeneous dispersion of nanoparticles in the epoxy resin and high interfacial bonding between nanoparticles and resin should exist.

By rheological measurement of nano-filled epoxy resins, not only changes in dispersion state of

\*Corresponding author: Hossein Hosseini, Department of Chemical Engineering, Abadan Branch, Islamic Azad University, Abadan, Iran, e-mail: hossein.hosseini@helsinki.fi

Behzad Shirkavand Hadavand: Institute for Color Science and Technology, Department of Resin and Additives, Tehran, Iran

nanoparticles in resin matrix but also interfacial bonding affected by surface modification can be examined. Dynamic mechanical analysis (DMA) is a technique that can provide a convenient and sensitive testing system for the determination of the thermo-mechanical properties of polymers as a function of frequency, temperature, or time. Some properties of polymers like the glass transition temperature and viscoelastic properties (storage modulus and loss modulus) can be achieved with the help of DMA [17–21]. Viscoelastic properties, such as storage modulus, loss modulus, and glass transition temperature, are evaluated to gauge the performance of the polymer film coating.

As the effect of nanoparticle type on viscoelastic properties of epoxy acrylate resins is an overlooked area, this issue is investigated in this research work. In this work, the temperature, which is dependent on the moduli of epoxy acrylate coatings filled with nanoparticles, was experimentally measured by DMA. The main objective is to attain a better understanding of the effect of Cu-Nano particles on the viscoelastic and thermal properties of UV-curable epoxy acrylate thin film.

## 2 Materials and methods

### 2.1 Materials

Epoxy resin (Epikote 828) with a molecular weight of 376 g/mol was purchased from Momentive Co. (OH, USA). Benzyltriethylammonium chloride (BTEAC) as catalyst, para methoxy phenol (PMP) as inhibitor, acrylic acid, vinyltrimethoxysilane (VTMS), triethoxy(methyl)silane (TEMS), benzophenone as photo initiator, isopropanol, and all acetone were supplied by Merck Company (Germany). Trimethylolpropane triacrylate (TMPTA) as a reactive diluent and triethanolamine (TEA) were purchased from Aldrich Company (USA). Nano CuO (40 nm) was produced by US Research Nanomaterials Inc. (USA). All the chemicals were used as received without any purification. Prepared nanocomposites were coated on glass substrate panels with dimensions of 150×100×3 mm.

### 2.2 Methods

#### 2.2.1 Modification of nano CuO

Nano CuO was dried in an oven to remove the adsorbed water. Fifty grams of dried nano CuO was added in 250 ml of isopropanol and sonicated for 10 min. Then, 2.5 g of

vinyl trimethoxysilane and 0.75 ml hydrochloric acid were added and mixed for 24 h by a magnetic stirrer at ambient temperature. Finally, the mixture was filtrated and washed with ethanol to remove the unreacted VTMS. The resulting product was dried at 60°C for 24 h. Modification of nano CuO with triethoxymethylsilane (TEMS) had the same procedure [22]. The structures of modified nano CuO are presented in Figure 1.

#### 2.2.2 Preparation of nanocomposite

The epoxy acrylate oligomer was synthesized by the reaction of epoxy resin (1 mol), acrylic acid (2 mol), benzyltriethylammonium chloride (BTEAC) as catalyst (1% w/w), and para-methoxy phenol (PMP) as inhibitor (0.1% w/w) that were poured in a glass container connected to the condenser and heated at 95°C for 4 h (Figure 2).

The formulation of UV-curable resin was achieved by 5% w/w benzophenone, triethanolamine, and 20% w/w trimethylolpropane triacrylate (TMPTA) as reactive diluents for adjusting the viscosity and 1, 3, and 5% w/w of nano CuO in total formulation. Formulated UV-curable compositions were applied on glass plates and then cured by UV radiation at ambient temperature. The properties of the films were evaluated after UV radiation curing.

### 2.3 Characterization techniques

Fourier transform infrared (FT-IR) spectra of the samples were performed in KBr disk on the Perkin Elmer (model Spectrum 1) spectrophotometer. All spectra scans were collected over the wave number range of 400–4000 cm<sup>-1</sup>. Thermal gravimetric analyzer (TGA) Pyris Diamond Perkin Elmer was used to study the thermal stability of the nanocomposites. Dried samples for TGA measurement were heated from 25°C to 600°C with a heating rate of 10°C/min under nitrogen flow. Differential scanning calorimetry

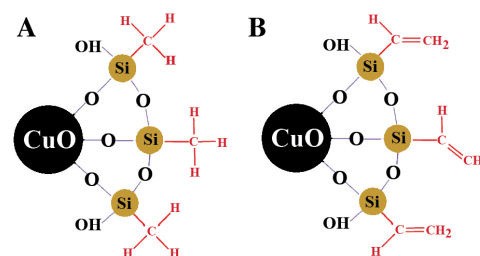


**Figure 1:** Modified nano CuO (A) with methyltriethoxysilane and (B) with vinyltrimethoxysilane.

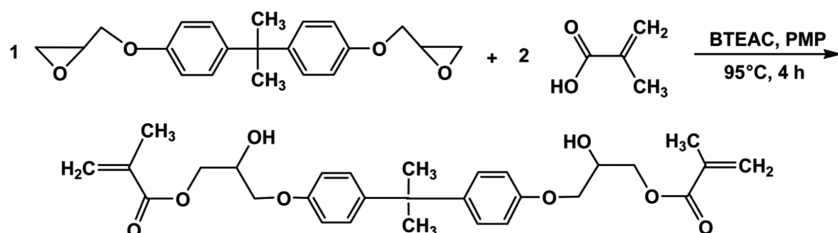


Figure 2: Preparation of epoxyacrylate.

(DSC) was performed with a Perkin Elmer model Pyris 6 using nitrogen atmosphere. The samples were heated in the temperature range of 25–400°C at a heating speed of 10°C/min. The response of the network to small strain mechanical deformation was measured as a function of temperature using dynamic mechanical thermal analyzer (DMTA) (Netzsch, DMA 242C Germany) in tensile mode. The morphology of the cured nanocomposite films were studied by field emission scanning electron microscope (FE-SEM), Hitachi S-4160.

## 3 Results and discussion

### 3.1 Characterization of nano CuO

FT-IR spectra of pure and modified nano CuO are presented in Figure 3. In the FT-IR spectra of pure nano CuO particle (Figure 3-1), a broad absorption band at 3659 cm<sup>-1</sup> confirms the OH groups on the surface of nano CuO. The peak at the region of 521 cm<sup>-1</sup> is attributed to the Cu-O stretching bond. The FT-IR spectra of modified CuO with TEMS and VTMS indicate the following characterization:

CuO-TEMS (Figure 3-2): 2972 cm<sup>-1</sup>: C-H stretching band, 1270 cm<sup>-1</sup>: CH<sub>3</sub>-Si(O-)<sub>3</sub>, 1128 cm<sup>-1</sup>: Si-O-Si, 1033 cm<sup>-1</sup>: (CH<sub>3</sub>)<sub>3</sub>

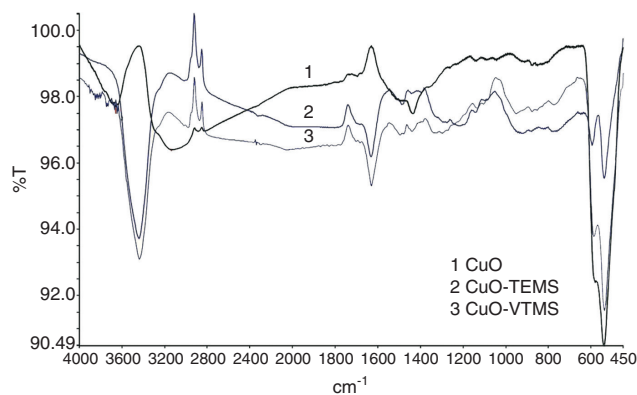


Figure 3: FT-IR spectra of pure and modified nano CuO.

Si-O-Si (CH<sub>3</sub>)<sub>3</sub>, 917 cm<sup>-1</sup>: Si-O-Cu, 780 cm<sup>-1</sup>: CH<sub>3</sub>-Si(O-)<sub>3</sub> and 540 cm<sup>-1</sup>: Cu-O.

CuO-VTMS (Figure 3-3): 2958 cm<sup>-1</sup>: C-H stretching band, 1408 and 1602 cm<sup>-1</sup>: Si-CH=CH<sub>2</sub>, 1276 cm<sup>-1</sup>: CH<sub>3</sub>-Si(O-)<sub>3</sub>, 1129 cm<sup>-1</sup>: Si-O-Si, 1045 cm<sup>-1</sup>: (CH<sub>3</sub>)<sub>3</sub> Si-O-Si (CH<sub>3</sub>)<sub>3</sub>, 965 cm<sup>-1</sup>: Si-O-Cu, 767 cm<sup>-1</sup>: CH<sub>3</sub>-Si(O-)<sub>3</sub> and 510 cm<sup>-1</sup>: Cu-O.

### 3.2 Epoxy-acrylate FT-IR

Figure 4 shows the FT-IR spectrum of epoxy-acrylate resin after curing. In Figure 4, the characteristic peak of O-H occurred at 3428 cm<sup>-1</sup>, and the strong absorption peak at 1059 cm<sup>-1</sup> was attributed to the stretching vibration of aromatic ether. The characteristic absorption peaks of 1515 cm<sup>-1</sup>, 1566 cm<sup>-1</sup>, and 1614 cm<sup>-1</sup> were attributed to the benzene ring, and the characteristic absorption peak of ester occurred at 1728 cm<sup>-1</sup>. The less characteristic absorption peaks occurred at 1614 cm<sup>-1</sup>, 1409 cm<sup>-1</sup>, and 809 cm<sup>-1</sup>; these were attributed to the stretching vibration of the C=C double bonds after they were completely cured. The polymer network structure was formed because of the double bond polymerization leading to the residual double bond being tied in the three-dimensional cross-linking network structure.

### 3.3 DSC results

Figures 5 and 6 demonstrated the comparison of the glass transition temperature for epoxy acrylate/nano-copper oxide and copper oxide nanoparticles modified with TEMS and VTMS. As we can see, for unmodified nano copper oxide, for a sample containing 3% CuO, the transition temperature increases to 99.3°C, and with increasing CuO to 5%, T<sub>g</sub> decreases to 95.8°C.

For samples with modified copper oxide, glass transition temperature is decreased with increasing CuO percent. These rates, from 1% to 3%, were the maximum. It may be for the particle size of nanocomposites, which increases the distance and flexibility of polymer chains;

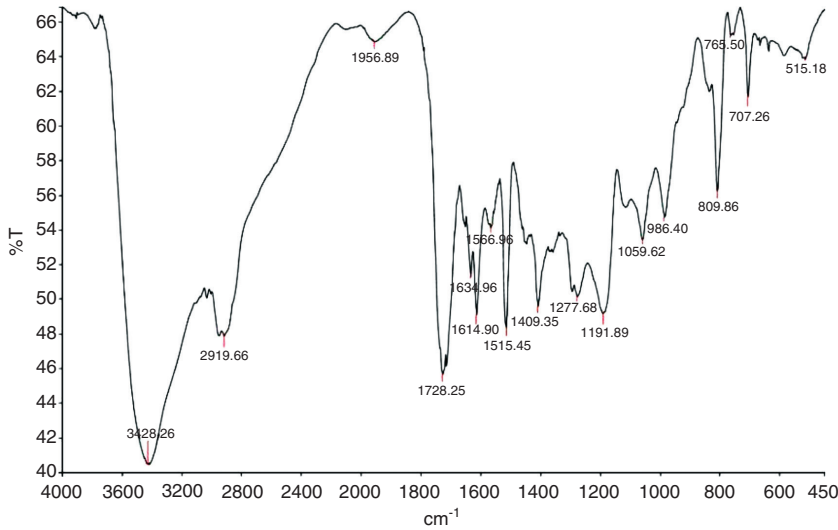


Figure 4: FT-IR spectrum of cured epoxy-acrylate.

therefore, the  $T_g$  is decreased. In higher percentage of nano-particles, the hard segment thereupon,  $T_g$  is increased.

In all modified nano copper oxide samples with a silane-coupling agent, glass transition temperature

relatively increases. It is related to the presence of silica in combination with a hard segment.

Increasing little amounts of the silane-coupling agent causes elasticity in the polymer chain because of the formation of the side chain in the backbone, and the glass transition temperature decreased. An increase in the amount of the silane-coupling agent because of the involvement of branches increases the glass transition temperature.

The comparison between the two types of coupling agents shows that the glass transition temperature in TEMS is more than that of VTMS. Epoxy acrylate with 1%, 3%, and 5% modified nano CuO-TEMS had glass transition temperatures of 103.3°C, 98°C, and 97.8°C, respectively. Glass transition temperatures for nano CuO modified with VTMS were 96.9°C, 94.47°C, and 96.6°C for 1%, 3%, and 5% nano CuO, respectively.

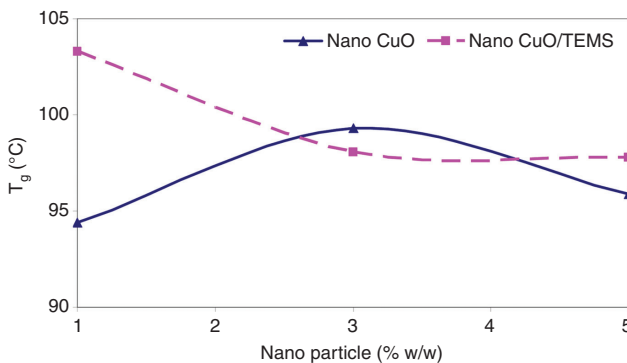


Figure 5: Glass transition temperature for epoxy acrylate/nanoCuO and CuO nanoparticles modified with TEMS.

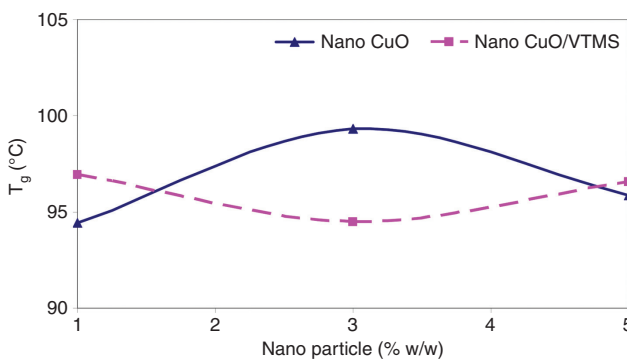


Figure 6: Glass transition temperature for epoxy acrylate/nanoCuO and CuO nanoparticles modified with VTMS.

### 3.4 Dynamic mechanical properties

DMA measures the deformation of a material in response to oscillating forces. In principle, the DMA technique detects the viscoelastic behavior of polymeric materials and yields quantitative results for the tensile storage modulus, and the corresponding loss modulus, the loss tangent, can then be expressed as the quotient of the loss and storage module. The loss modulus quantifies the energy that is converted to heat during deformation of the material. With increasing flexibility of the composites,  $T_g$  is decreased. A dynamic mechanical analyzer was used for measuring the temperature-dependent elastic and loss moduli of the

cured epoxy-acrylate nanocomposites (Figures 7 and 8). The maximum of the  $\tan \delta$  curve corresponds to the glass transition temperature above when significant chain motion takes place, as shown in Figure 8. Damping is an increasing important factor in the design of structures to minimize structural instability and fatigue failure of advanced composites. Materials with high stiffness generally have low damping.

In the EA-CuO (5 wt%) sample, increase in storage modulus in comparison with 1 and 3 wt% samples is due to better attachment of polymer and filler. In EA-CuO (1%)-TEMS, the storage modulus is higher than the EA-CuO (1%)-VTMS and EA-CuO (1%) due to the better attachment

of the EA-CuO-TEMS sample. In EA-CuO (3%)-VTMS, the storage modulus is higher than the EA-CuO-TEMS and EA-CuO samples because of better attachment of the filler and the polymer in this sample in comparison to similar samples. This observation can be seen for 5% samples, too. Therefore, in a high filler percent, it is favorable to use EA-CuO-VTMS sample due to its better attachment. An improvement in composite stiffness can be seen in EA-CuO (3%)-VTMS because 3% is the percolation threshold of the filler, and 5% passes this threshold. In EA-CuO-TEMS with increase in filler percent, storage modulus decreases, and better composite stiffness is observed in the 1% sample, which shows that the percolation threshold of the filler is 1% in this sample. The EA-CuO sample has higher composite stiffness in samples with 5% filler content. While passing from glass state to rubber state, temperature increase results in lower storage modulus. Then, the best mechanical-dynamical properties of composite in the EA-CuO sample can be seen in the 5% filler. The same finding can be seen in the EA-CuO-TEMS sample with 1% filler, but in the EA-CuO-VTMS sample, this result can be seen in the 3% sample. In the investigation of loss moduli changes with temperature, one can find a softening point and relaxation changes. Loss tangent, which is the proportion of loss modulus to storage modulus, is related to molecular movements and phase transitions and is indicative of attachment between polymer network interface and filler in composites. In EA-CuO, the increase in fillers above 3% results in a decrease in  $T_g$  due to the higher flexibility of the composite. EA-CuO-VTMS with 3% filler has the lowest  $T_g$  and the highest flexibility. In contrast, EA-CuO-TEMS with 5% filler has the highest

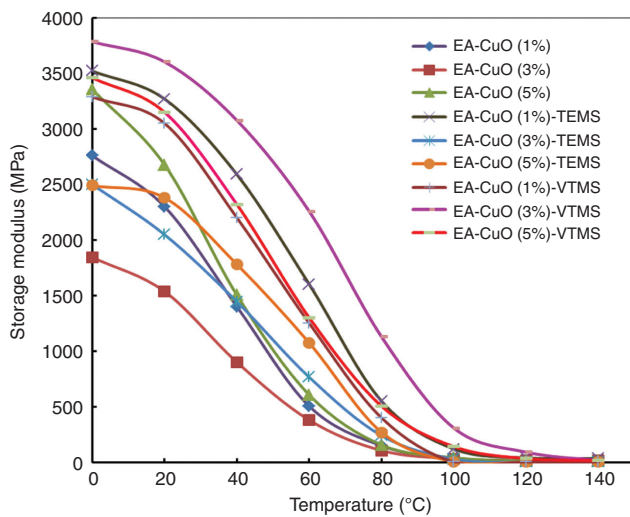


**Figure 7:** Storage modulus of epoxy-acrylate nanocomposites measured by DMA.

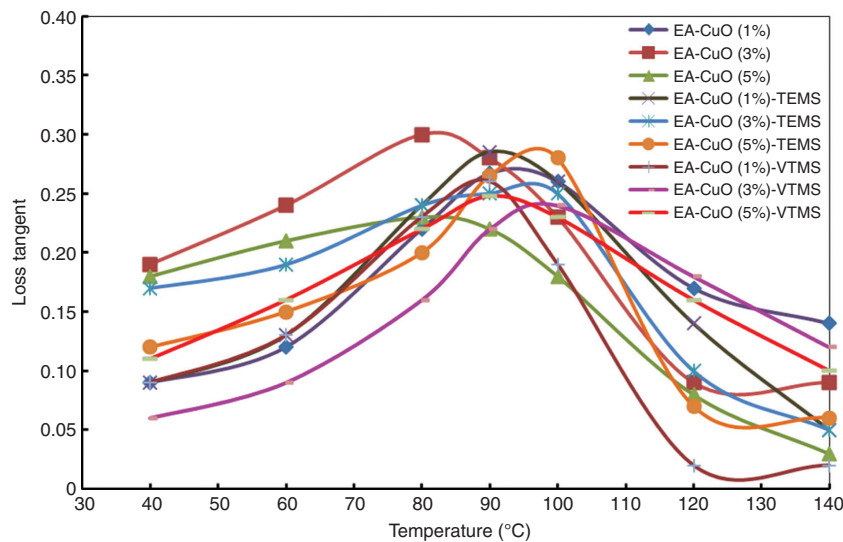


**Figure 8:** Loss tangent of epoxy-acrylate nanocomposites measured by DMA.

flexibility. In EA-CuO, the widest loss tangent peak is related to 5%, suggesting a more heterogeneous material. The same observation can be seen for EA-CuO-VTMS with 5% filler. But in the case of EA-CuO-TEMS, the widest loss tangent peak is found in the sample with 3% filler. Therefore, the relaxation mode in this sample is higher than those of the 1% and 5% samples. Furthermore, there is a significant shift in the  $T_g$  from 55°C for neat resin to 92°C, 96.3°C, and 97°C for 1, 3, and 5 wt% CuO-TEMS, respectively, as determined by the maxima of the  $\tan \delta$  peaks (Figure 8).  $T_g$  is important for establishing a maximal temperature for use, that is, a material operational limit.

### 3.5 Thermogravimetric analysis of nanocomposites

Thermogravimetric analysis measures changes in weight that occur to a sample as a function of temperature over time. Because of the sensitivity of TGA to experimental conditions, a strict comparison of thermal stability can only be achieved by analyzing samples of interest under identical conditions. The thermographs results of the epoxy acrylate containing nano CuO, nano CuO+TEMS, and nano CuO+VTMS are shown in Table 1. Figure 9 demonstrates the comparison of cured nanocomposite film for 3% w/w of nanoparticle. In Figure 9, there is a slight drop in the curves around 110°C that is related to evaporation of water, solvent, and unreacted monomers. Also, severe reduction and weight loss was observed at the temperature around 300°C, which is related to the degradation of the polymer chain. As is evident in Figure 9, the polymer is completely degraded around the temperature of 520°C. There is a slight difference between the thermograph of the modified and unmodified samples at around

**Table 1:** Results of thermogravimetric analysis for epoxy acrylate containing nano CuO, nano CuO+TEMS, and nano CuO+VTMS.

Samples	Temperature (°C) and lost weight (%)				
	$T_{0\%}$	$T_{5\%}$	$T_{50\%}$	$T_{75\%}$	$T_{Max}$
Blank	25	208.35	445.93	494.51	535.76
CuO 1%	25	209.76	443.84	502.92	533.07
CuO 3%	25	219.82	445.54	494.80	530.97
CuO 5%	25	197.70	438.27	487.02	524.54
CuO-TEMS 1%	25	209.50	445.28	504.62	532.12
CuO-TEMS 3%	25	194.63	434.15	482.97	525.34
CuO-TEMS 5%	25	211.08	438.26	489.14	523.46
CuO-VTMS 1%	25	203.03	447.53	505.37	508.85
CuO-VTMS 3%	25	212.85	440.95	489.82	505.50
CuO-VTMS 5%	25	198.81	440.13	493.76	503.74

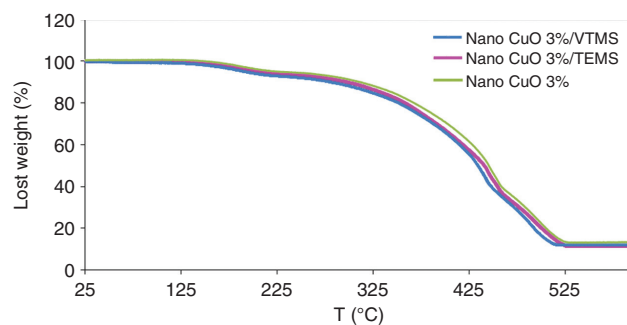


**Figure 9:** Comparison of TGA graph of epoxy acrylate containing 3% w/w nano CuO, nano CuO+TEMS, and nano CuO+VTMS.

220–300°C that is related to the decomposition of organic parts of silane-coupling agents. In general, it could be concluded that the prepared samples are stable until reaching around 300°C, and separation of the organic parts of silane-coupling agents started at a temperature of 220°C, and this procedure is similar in all groups of nanocomposites.

### 3.6 Morphology of nanocomposites

The effects of modification in the dispersion of the nanoparticles were studied using field emission scanning electron microscopy (FE-SEM). Figure 10 presents the FE-SEM images of the surface morphology for blank films (A) and films with 3% nano CuO (B), 3% nano CuO modified with TEMS (C), and VTMS (D). From the images, it is clear that the best dispersion is for the sample with nano CuO modified with VTMS. The exits of C=C bond in CuO modified with VTMS participate in the radical polymerization of the curing process to achieve uniform dispersion. In the samples with CuO modified with TEMS, because of their organic parts, we can see less agglomeration than the none-modified CuO, and dispersion status is better but not the same as the nano CuO modified with VTMS films.

## 4 Conclusions

In this paper, a series of UV curable epoxy-acrylate nanocomposite with high storage modulus was developed. The nanocomposite contains silane-modified CuO nanoparticles, epoxy-acrylate resin, abstraction type photoinitiator, reactive diluent, and catalyst. It was found that modification of CuO nanoparticles improves the dispersion of the nanoparticles, and the best dispersion was for the nanoparticles modified with VTMS. Silane compound acts as

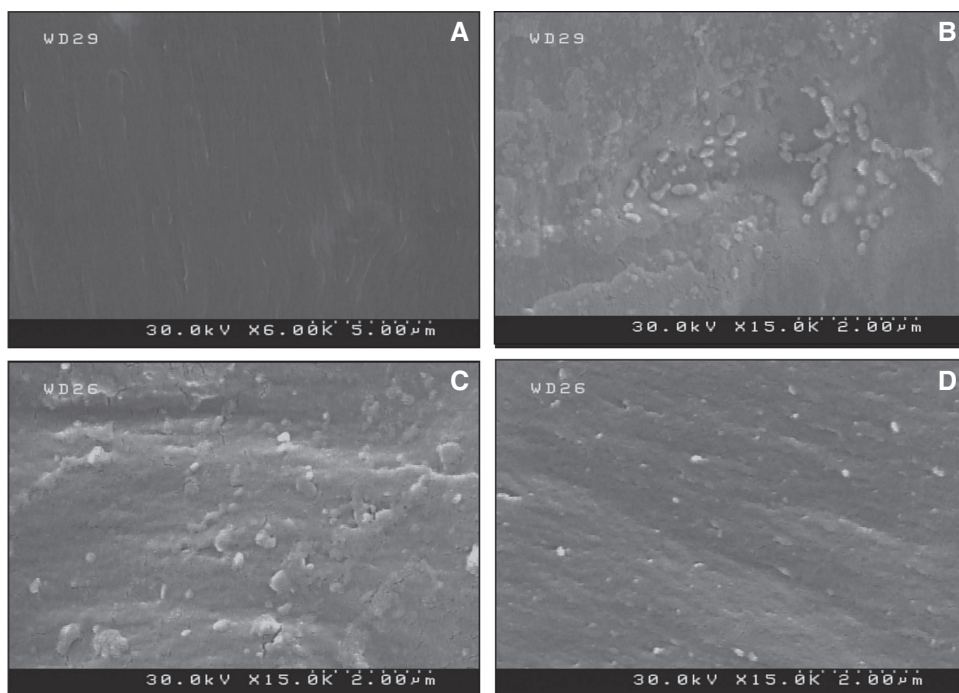


**Figure 10:** FE-SEM images of epoxy-acrylate nanocomposites. (A) Blank, (B) 3% w/w CuO, (C) 3% w/w CuO+TEMS, and (D) 3% w/w CuO+VTMS.

a coupling agent between CuO nanoparticles and the polymer matrix. The FT-IR analysis shows that the percentage conversion of double bonds in the UV-cured coating was found to be very high, which suggest a very high degree of curing of formulations via the UV-curing process resulting in the formation of the high-performance coatings. TGA results show that the prepared samples are stable until reaching around 300°C, and the separation of the organic parts of the silane-coupling agents started at a temperature of 220°C. The results indicated that the UV-curable epoxy acrylate-CuO modified nanocomposites, showing good mechanical properties and thermal behavior.

**Acknowledgments:** This study was partially supported by the Research Department of Abadan Branch of Islamic Azad University. The authors are grateful for the support.

## References

- [1] Fischer F, Beier U, Wolff-Fabris F, Altstadt V. *Sci. Eng. Compos. Mater.* 2011, 18, 209–215.
- [2] Fan HB, Yuen MMF. *Polymer* 2007, 48, 2174–2178.
- [3] Jung SJ, Lee SJ, Cho WJ, Ha CS. *J. Appl. Polym. Sci.* 1998, 69, 695–708.
- [4] Zou K, Soucek MD. *Macromol. Chem. Phys.* 2004, 205, 2032–2039.
- [5] Chattopadhyay DK, Panda SS, Raju KVS. *Prog. Org. Coat.* 2005, 54, 10–19.
- [6] O'Brien DJ, Mather PT, White SR. *J. Compos. Mater.* 2001, 35, 883–904.
- [7] Chen Z, Wu JF, Fernando S, Jagodzinski K. *Prog. Org. Coat.* 2011, 71, 98–109.
- [8] Mohtadzadeh F, Zohuriaan-Mehr MJ, Shirkavand Hadavand B, Dehghan A. *Prog. in Org. Coat.* 2015, 89, 231–239.
- [9] Najafi F, Bakhshandeh E, Shirkavand Hadavand B, Saeb MR. *Prog. Org. Coat.* 2014, 77, 1957–1965.
- [10] Farzad H, Najafi F, Bengisu M, Yilmaz E, Shirkavand Hadavand B. *J. Macromol. Sci. A.* 2013, 50, 504–512.
- [11] Zotti A, Borriello A, Martone A, Antonucci V, Giordano M, Zarrelli M. *Compos. B: Eng.* 2014, 67, 400–409.
- [12] Omrania A, Simon LC, Rostami A. *Mater. Chem. Phys.* 2009, 114, 145–150.
- [13] Zhang X, Alloul O, He Q, Zhu J, Verde MJ, Li Y, Wei S, Guo Z. *Polymer* 2013, 54, 3594–3604.
- [14] Shirkavand Hadavand B, Mahdavi Javid K, Gharagozlou M. *Mater. Des.* 2013, 50, 62–67.
- [15] Wang K, Chen L, Wu J, Toh ML, He C, Yee AF. *Macromolecules* 2005, 38, 788–800.
- [16] Gojny FH, Wichmann MHG, Fiedler B, Schulte K. *Compos. Sci. Technol.* 2005, 65, 2300–2313.
- [17] Jones DS, Tian Y, Abu-Diak O, Andrews GP. *Adv. Drug Deliv. Rev.* 2012, 64, 440–448.
- [18] Montazeri A, Montazeri N. *Mater. Des.* 2011, 32, 2301–2307.
- [19] Montazeri A, Pourshamsian K, Riazian M. *Mater. Des.* 2012, 36, 408–414.
- [20] Perfetti G, Jansen KMB, Wildeboer WJ, Hee P, Meesters GMH. *Int. J. Pharm.* 2010, 384, 109–119.
- [21] Fogelstrom L, Malmstrom E, Johansson M, Hult A. *Appl. Mater. Inter.* 2010, 2, 1679–1684.
- [22] Shirkavand Hadavand B, Ataefard M, Fakhrazadeh Bafghi H. *Compos. B Eng.* 2015, 82, 190–195.